Equalized Net Diffusion (END) in Image Denoising

SEONGJAI KIM
Mississippi State University
Department of Mathematics & Statistics
Mississippi State, MS 39762 USA

Abstract: This article is concerned with the method of diffusion modulation, which can be applied for various conventional partial differential equation (PDE)-based restoration models in order to effectively restore not only fine structures but also slow transitions. We in particular introduce the *equalized net diffusion* (END) which tries to equalize the anisotropic diffusion over a wide range of image content. Although the new reformulated models incorporating END are highly nonlinear, they can be simulated efficiently by adopting linearized stable numerical procedures. The END-incorporated models have outperformed over the basic (conventional) PDE-based models in both quality and efficiency.

Key-Words: Image restoration, variational approach, diffusion modulation, equalized net diffusion, PDE-based image denoising.

1 Introduction

Image denoising is an important step for various image-related applications and is often necessary as a pre-processing for other imaging techniques such as segmentation, registration, and visualization. Thus image denoising methods have occupied a peculiar position in image processing, computer graphics, and their applications [5, 10]. A considerable research has been carried out for the theoretical and computational understanding of *partial differential equation* (PDE)-based denoising models such as the Perona-Malik model [12], the total variation (TV) model [13], and their variants [1, 2, 3, 15]. However, most of those PDE-based denoising models may lose fine structures and "natural look", during the restoration, due to an undesired dissipation and/or a tendency of converging to a piecewise constant image.

In this article, we will introduce the method of diffusion modulation in order to significantly reduce the artifacts and efficiently suppress the noise. In particular, we will study a new mathematical formulation such as the *equalized net diffusion* (END). The objective in this article is to develop an effective (non-variational) restoration model which can restore fine structures and slow transitions as well. Note that the set of PDEs derived from variational approaches is much smaller than the set of all available diffusion-like PDEs.

The article is organized as follows. In Section 2, we briefly review conventional PDE-based models in image denoising: variational approaches followed by their non-variational variants. Section 3 begins with analyzing sources of undesired dissipation of conventional PDE-based models. The same section presents the END reformulation. In Section 4, numerical examples are presented to show effectiveness of the new END reformulation. Section 5 concludes our development and experiments. It has been numerically verified that the END reformulation can restore fine structures satisfactorily, outperforming over the basic (conventional) PDE-based models in both quality and efficiency.

In this article, images are considered as discrete functions having real-values between 0 and 1 (by scaling by a factor of 1/255). After processing, they will be scaled back for the 8-bit display.

2 Preliminaries

This section reviews briefly variational approaches in image denoising and their non-variational variants.

Let u_0 be an observed image of the form

$$u_0 = u + v, \tag{1}$$

where u is the desired image and v denotes the noise having a zero mean. Then a common denoising tech-

nique is to minimize a functional of gradient:

$$u = \arg\min_u \Big\{ \int_\Omega \rho(|\nabla u|)\, d\mathbf{x} + \frac{\lambda}{2} \int_\Omega (u_0 - u)^2\, d\mathbf{x} \Big\}, \tag{2}$$

where Ω is the image domain, ρ is an increasing function (often, convex), and $\lambda \geq 0$ denotes the constraint parameter. It is often convenient to transform the minimization problem (2) into a differential equation, called the *Euler-Lagrange equation*, by applying the variational calculus [14]:

$$-\nabla \cdot \Big(\rho'(|\nabla u|) \frac{\nabla u}{|\nabla u|} \Big) = \lambda\, (u_0 - u). \tag{3}$$

For an edge-adaptive image denoising, it is required to hold $\rho'(x)/x \to 0$ as $x \to \infty$.

For a convenient numerical simulation of (3), the energy descent direction may be parameterized by an artificial time t. That is, u can be considered as an evolutionary function and the corresponding evolutionary equation can be obtained by adding $\frac{\partial u}{\partial t}$ on the left side of (3).

When $\rho(x) = x$, the model (3) in its evolutionary form becomes the total variation (TV) model [13]:

$$\frac{\partial u}{\partial t} - \kappa(u) \;=\; \lambda(u_0 - u), \qquad \text{(TV)} \tag{4}$$

where $\kappa(u)$ is the *mean curvature* defined as

$$\kappa(u) = \nabla \cdot \Big(\frac{\nabla u}{|\nabla u|} \Big).$$

It is often the case that the constraint parameter λ is set as a constant, as suggested by Rudin-Osher-Fatemi [13]. In order to find the parameter, the authors merely multiplied (4) by $(u_0 - u)$ and averaged the resulting equation over the whole image domain Ω. Then, for its state state,

$$\lambda = -\frac{1}{\sigma^2} \frac{1}{|\Omega|} \int_\Omega (u_0 - u)\, \kappa(u)\, d\mathbf{x}, \tag{5}$$

where σ^2 is the noise variance.

Most of conventional PDE-based restoration models have shown either to converge to a piecewise constant image or to lose fine structures of the given image. For example, the TV model tends to converge to a piecewise constant image. Such a phenomenon is called the *staircasing effect*. In order to suppress it, Marquina and Osher [9] suggested to multiply the stationary TV model by a factor of $|\nabla u|$:

$$\frac{\partial u}{\partial t} - |\nabla u|\, \kappa(u) \;=\; \lambda\, |\nabla u|\, (u_0 - u). \quad \text{(ITV)} \tag{6}$$

Since $|\nabla u|$ vanishes only on flat regions, its steady state is analytically the same as that of the TV model (4). We will call (6) the *improved TV* (ITV) model, as called in [11]. Such a non-variational reformulation turns out to reduce the staircasing effect successfully; however, it is yet to be improved for a better preservation of fine structures.

To form another variant, we set $\rho(x) = x^{2-q}$, $0 \leq q < 2$, in (3) and multiply the resulting equation by $|\nabla u|^q$ [8]:

$$\frac{\partial u}{\partial t} - |\nabla u|^q\, \nabla \cdot \Big(\frac{\nabla u}{|\nabla u|^q} \Big) = \beta\, (u_0 - u), \quad \text{(CCAD)} \tag{7}$$

where $\beta = \lambda\, |\nabla u|^q / (2 - q)$. The second-order differential operator in (7) turns out to be closely related to that of the Perona-Malik model [12], in particular when $q \to 2$. Thus we will call (7) the *convex-concave anisotropic diffusion* (CCAD). The CCAD model can be implemented as a *stable* numerical algorithm for all $q \in [0, 2)$ [8]. It has been numerically verified that for $1 < q < 2$, the CCAD model is superior to the ITV model, a CCAD model with $q = 1$.

Now, we will consider a way of choosing a variable constraint parameter for e.g. the TV model, which has motivated the method of diffusion modulation to be presented in the next section.

As an alternative to (5), one can get a variable parameter $\lambda = \lambda(\mathbf{x})$ by averaging *locally*:

$$\lambda(\mathbf{x}) = -\frac{1}{\sigma_{\mathbf{x}}^2} \frac{1}{|\Omega_{\mathbf{x}}|} \int_{\Omega_{\mathbf{x}}} (u_0 - u)\, \kappa(u)\, d\mathbf{x},$$

where $\Omega_{\mathbf{x}}$ is a neighborhood of $\mathbf{x}$ and $\sigma_{\mathbf{x}}^2$ denotes the local noise variance measured over $\Omega_{\mathbf{x}}$. Then, the right side of the above equation can be approximated as

$$\lambda(\mathbf{x}) \approx \frac{1}{\sigma_{\mathbf{x}}^2} \, \|u_0 - u\|_{\mathbf{x}} \cdot \|\kappa(u)\|_{\mathbf{x}}, \tag{8}$$

where $\|\cdot\|_{\mathbf{x}}$ denotes a local average over $\Omega_{\mathbf{x}}$. Thus the TV model (4), when its stationary equation is scaled by $1/\|\kappa(u)\|_{\mathbf{x}}$ and regularized by a constant $\varepsilon_0 > 0$, can be rewritten as

$$\frac{\partial u}{\partial t} - \frac{1}{\|\kappa(u)\|_{\mathbf{x}} + \varepsilon_0}\, \kappa(u) = \frac{1}{\sigma_{\mathbf{x}}^2}\, \|u_0 - u\|_{\mathbf{x}}\, (u_0 - u). \tag{9}$$

The steady state of (9) must be essentially the same as that of the TV model (4) incorporating (8), when ε_0 is small. However, in practice, their numerical solutions differ a lot from each other. Note that the numerical simulation is usually terminated much earlier

than reaching the steady state. The non-variational reformulation (9) is more *explicit and direct* than the original variational model (4), in the control of both diffusion and constraint.

Note that the above explicit reformulation (9) can be applied for various other models including the ITV model (6) and the CCAD model (7).

3 The Method of Diffusion Modulation

In this section, we will present the method of diffusion modulation, introducing an effective denoising model which consists of three components: the diffusion operator, the modulator, and the constraint term. We first analyze sources of undesired dissipation for conventional PDE-based denoising models.

3.1 Sources of undesired dissipation

For simplicity, we exemplify the TV model (4); its corresponding noise (residual) is $v = u_0 - u$. Thus, it follows from (4) the associated *residual equation*

$$\frac{\partial v}{\partial t} + \lambda\, v = -\kappa(u). \tag{10}$$

Although the given image u_0 is piecewise smooth and is the same as the desired image at $t = 0$, i.e., $v(t = 0) \equiv 0$, the residual at $t > 0$ becomes positive or negative at pixels where the image is concave or convex, respectively. Thus the solution of the TV model at $t > 0$, $u(t) = u_0 - v(t)$, must involve undesired dissipation wherever its curvature is nonzero; the larger the curvature is (in modulus), the more undesired dissipation occurs.

The above observation for the TV model can be applied to PDE-based denoising models of the form

$$\frac{\partial u}{\partial t} + Su \;=\; Q(u_0 - u), \tag{11}$$

where S is a diffusion operator and Q denotes a non-negative constraint term. (With appropriate choices of S and Q, the model (11) can express most of denoising models, including aforementioned ones.)

We summarize the observation as follows: *The solution of* (11) *must incorporate more undesired dissipation at pixels where the diffusion magnitude* $|Su|$ *is larger*. This is an unwanted property and a major source of undesired dissipation for conventional PDE-based denoising models, with which fine structures can be easily deteriorated.

3.2 The equalized net diffusion (END)

In order to overcome the drawback of conventional PDE-based models, we may consider the following reformulation of (11), of which the diffusion operator is explicitly modulated by a function of diffusion operator itself:

$$\frac{\partial u}{\partial t} + M(Su)\, Su \;=\; R\,(u_0 - u), \tag{12}$$

where M is a positive function (a modulator) and R denotes an appropriate constraint term. We will call $M(Su)\, Su$ the *net diffusion* of the model (12), and denote it by $N(Su)$.

The purpose of the modulator M is to suppress the undesired excessive dissipation at pixels of large diffusion magnitude $|Su|$; a strategy will be discussed below.

An effective modulator can be defined to impose the net diffusion *approximately equal* over a wide range of $|Su| \geq s_0 > 0$, for some s_0. However, the net diffusion function $N(s)\,(:= M(s)s)$ must be increasing and origin-symmetric. Note that the model (12) converges in the direction in which the net diffusion decreases (in modulus); the convergence must introduce denoising, i.e., Su becomes smaller (in modulus); which requires N to be increasing. The origin-symmetry of N implies that $N(-s) = -N(s)$, with which N becomes equally diffusive for both concavities (up and down). Such an equalized net diffusion (END) function can be defined e.g. as

$$N(s) = M(s)s = \frac{\gamma}{1 + \eta\,|s|}\, s, \tag{13}$$

for some positive constants η and γ. See Figure 1, where $|N(s)|$ evaluates (almost) the same values except on smooth regions (where $|s|$ is small) and therefore the function N may introduce an *equalized* net diffusion in practice. Incorporating (13), the model (12) can be rewritten as follows:

$$\frac{\partial u}{\partial t} + \frac{\gamma}{1 + \eta\,|Su|}\, Su \;=\; R\,(u_0 - u). \quad \text{(END)} \tag{14}$$

We will call it the *equalized net diffusion* (END) model of (11).

Remark. The above *method of diffusion modulation* is not completely new. The ITV model is based on such a method in which the diffusion is modulated to suppress the staircasing effect. On the other hand, END reformulates the regularization framework in order to preserve not only fine structures but also slow

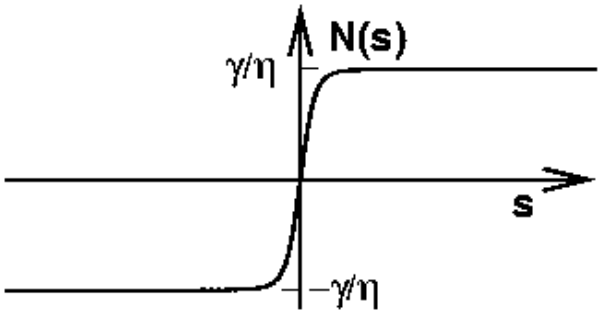

Fig. 1. The net diffusion function $N(s)$ in (13) for some choices of η and γ.

transitions satisfactorily. Note that the END model is no longer conservative, i.e., there is no mathematical guarantee that the average gray value of the input image is the same as that of the outcome. However, since the conventional PDE-based models tend to lose fine structures (Section 3.1) and easily introduce undesired dissipation, the END model has resulted in superior images; see numerical experiments in Section 4.

3.3 Parameters η and γ

In the remainder of the section, we will consider a strategy for the selection of appropriate η and γ. Let u^{n-1} be the solution in the last time level. Then the constants η and γ for the computation of u^n can be determined as

$$\begin{aligned} &\text{(a)} \quad N(T) = \chi \frac{\gamma}{\eta}, \quad 0 < \chi < 1, \\ &\text{(b)} \quad M(T) = 1, \end{aligned} \tag{15}$$

for some threshold $T > 0$. The equation (15.a) determines the sharpness of N near the origin; it becomes sharper, as $\chi \to 1$. On the other hand, (15.b) implies

$$\begin{aligned} &|N(s)| < |s| \quad \text{for } |s| > T, \\ &|N(s)| > |s| \quad \text{for } |s| < T. \end{aligned} \tag{16}$$

Thus the net diffusion, $N(Su)$, is smaller than the original diffusion (Su) at pixels where the image content changes rapidly ($|Su| > T$), while it becomes enlarged on slow transitions.

The equations in (15) can be easily solved for η and γ, as follows:

$$\eta = \frac{\chi}{1-\chi} \cdot \frac{1}{T}, \qquad \gamma = 1 + \eta T = \frac{1}{1-\chi}. \tag{17}$$

Then, it follows from the above that

$$T \le |N(s)| \le \frac{\gamma}{\eta} = T \frac{1}{\chi}, \quad \text{for } |s| \ge T. \tag{18}$$

Thus the net diffusion on oscillatory regions ($|Su| \ge T$) can differ only by a factor of $1/\chi$. The parameter χ must be large enough to try to equalize the net diffusion on oscillatory regions; however, it should not be too large, because otherwise the (almost flat) net diffusion will hardly be effective in denoising. We will set $\chi = 0.85 \sim 0.95$.

The threshold T must be small enough to equalize the net diffusion on every interesting oscillatory region including edges and textures. It has been numerically verified that T can be chosen to be an average of $|Su|$, S_0:

$$T = S_0 := \Big(\frac{1}{|\Omega|} \int_\Omega |Su|^2 \, d\mathbf{x} \Big)^{1/2}. \tag{19}$$

Since the diffusion magnitude $|Su|$ evaluated from oscillatory regions is typically larger than the L^2-average S_0, the threshold T in (19) suffices to equalize the net diffusion for regions of fine structures. For example, for $Su = -|\nabla u|^q \nabla \cdot (\nabla u / |\nabla u|^q)$, $0 \le q < 2$, the average S_0 is often evaluated between 0.01 and 0.3 for typical natural images. (The images have been scaled to have values in $[0, 1]$.) Let $S_0 = 0.1$ and select $\chi = 0.9$. Then it follows from (17), (18), and (19) that $\eta = 90$, $\gamma = 10$, and

$$0.1 \le |N(s)| \le 0.111\cdots, \quad \text{for } |s| \ge S_0 = 0.1.$$

Note that the choice of T in (19) keeps an average of the modulator M to be one.

The above arguments for the choice of η and γ can be summarized as follows:

1. *Select a constant* χ, $0 < \chi < 1$.
2. *Compute the* L^2*-average of* $|Su|$, S_0*:*

$$S_0 = \Big(\frac{1}{|\Omega|} \int_\Omega |Su|^2 \, d\mathbf{x} \Big)^{1/2}. \tag{20}$$

3. *Compute the parameters* η *and* γ*:*

$$\eta = \frac{\chi}{1-\chi} \cdot \frac{1}{S_0}, \qquad \gamma = \frac{1}{1-\chi}. \tag{21}$$

Thus END requires the user to select only a single parameter, χ, which determines the sharpness of the net diffusion function N. (One can set $\chi = 0.85 \sim 0.95$, in practice.) With the resulting parameters η and γ, the average of the diffusion modulator M becomes one (independently on the selection of χ, $0 < \chi < 1$). Note that when $\chi = 0$, we have $M(s) \equiv 1$ and therefore the END model (14) turns out to be the conventional model (11).

(a) (b)

Fig. 2. The Lenna: (a) The original image and (b) a noisy image contaminated by a Gaussian noise of PSNR=22.8 (dB).

Table 1. A PSNR analysis.

	$q = 0.0$	$q = 0.5$	$q = 1.0$	$q = 1.4$	$q = 1.8$
CCAD[q]	27.0	27.2	27.8	28.2	28.3
END-CCAD[q]	29.8	29.8	30.1	30.2	30.3

4 Numerical Experiments

For numerical experiments, we select CCAD (7) for the basic model; in its END-incorporated model (14), we set $\chi = 0.9$. The constraint parameters β and R, respectively in (7) and (14), are chosen utilizing the so-called *texture-free residual* parameterization suggested in [8]. For an efficient simulation of the models, we adopt an incomplete Crank-Nicolson alternating direction implicit (CN-ADI) time-stepping iterative procedure [4, 7]. The CN-ADI iteration is stopped along with the stopping criterion:

$$\|u^n - u^{n-1}\|_\infty < 0.01.$$

For simplicity, the noise is considered to be Gaussian.

To show effectiveness of the new model, we begin with the Lenna image, as depicted in Figure 2. A Gaussian noise of PSNR=22.8 (dB) is incorporated into Figure 2(b). In the following, the CCAD model with a selected q will be denoted by CCAD[q] and its corresponding END model by END-CCAD[q].

Table 1 presents PSNRs for the restored images, from Figure 2(b), by CCAD[q] and END-CCAD[q] for various q's. Note that CCAD[0] becomes the linear heat equation, while CCAD[1] is the ITV model (6). The CCAD model can restore a better image as q increases; it has been numerically verified that the best result can be obtained when $q = 1.5 \sim 1.9$. As one can see from the table, the END reformulation has improved the restoration quality more dramatically than different choices of basic models. Note that the PSNR of END-CCAD[0], the END-incorporated linear heat flow, is larger than those of all CCAD models (not incorporating END). In practice, the END incorporation increases the computational cost by 30-50% per iteration. However, the END models have converged in 2-5 CN-ADI iterations for all cases we have tested (including those not presented in this article); the END reformulation is often more efficient.

See [6] for more examples and analysis which demonstrate effectiveness of the END reformulation.

5 Conclusions

Conventional PDE-based restoration models may lose important fine structures, during image denoising. In

order to significantly reduce the artifacts, we have studied the method of diffusion modulation, particularly the *equalized net diffusion* (END). The reformulated models incorporating END are highly nonlinear; however, they can be implemented as a stable and efficient computational algorithm by applying linearized Crank-Nicolson alternating direction implicit (CN-ADI) method. It has been numerically verified that the newly reformulated models can restore not only fine structures but also slow transitions satisfactorily, just in 2-5 linearized CN-ADI iterations, outperforming over the conventional PDE-based restoration models in both quality and efficiency.

Acknowledgment

The work of the author is supported in part by NSF grants DMS-0630798 and DMS-0609815.

References:

[1] L. Alvarez, P. Lions, and M. Morel, "Image selective smoothing and edge detection by nonlinear diffusion. II," *SIAM J. Numer. Anal.*, vol. 29, pp. 845–866, 1992.

[2] M. J. Black, G. Sapiro, D. H. Marimont, and D. Heeger, "Robust anisotropic diffusion," *IEEE Trans. Image Processing*, vol. 7, no. April, pp. 421–432, 1998.

[3] F. Catte, P. Lions, M. Morel, and T. Coll, "Image selective smoothing and edge detection by nonlinear diffusion." *SIAM J. Numer. Anal.*, vol. 29, pp. 182–193, 1992.

[4] Y. Cha and S. Kim, "Edge-forming methods for color image zooming," *IEEE Trans. Image Process.*, vol. 15, no. 8, pp. 2315–2323, 2006.

[5] R. Gonzalez and R. Woods, *Digital Image Processing, 2nd Ed.* Upper Saddle River, New Jersey: Prentice-Hall, Inc., 2002.

[6] S. Kim, "Image restoration via equalized net diffusion," (preprint).

[7] ——, "PDE-based image restoration: A hybrid model and color image denoising," *IEEE Trans. Image Processing*, vol. 15, no. 5, pp. 1163–1170, 2006.

[8] S. Kim and H. Lim, "A non-convex diffusion model for simultaneous image denoising and edge enhancement," *Electronic Journal of Differential Equations*, 2006, (accepted).

[9] A. Marquina and S. Osher, "Explicit algorithms for a new time dependent model based on level set motion for nonlinear deblurring and noise removal," *SIAM J. Sci. Comput.*, vol. 22, pp. 387–405, 2000.

[10] S. Mitra and G. Sicuranza, *Nonlinear Image Processing*. San Diego, San Francisco, New York, Boston, London, Sydney, ToKyo: Academic Press, 2001.

[11] S. Osher and R. Fedkiw, *Level Set Methods and Dynamic Implicit Surfaces*. New York: Springer-Verlag, 2003.

[12] P. Perona and J. Malik, "Scale-space and edge detection using anisotropic diffusion," *IEEE Trans. on Pattern Anal. Mach. Intell.*, vol. 12, pp. 629–639, 1990.

[13] L. Rudin, S. Osher, and E. Fatemi, "Nonlinear total variation based noise removal algorithms," *Physica D*, vol. 60, pp. 259–268, 1992.

[14] R. Weinstock, *Calculus of Variations*. New York: Dover Pubilcations, Inc., 1974.

[15] Y.-L. You, W. Xu, A. Tannenbaum, and M. Kaveh, "Behavioral analysis of anisotropic diffusion in image processing," *IEEE Trans. Image Process.*, vol. 5, pp. 1539–1553, 1996.